Studies of polarimetric properties of lunar surface using Mini-SAR data

Shiv Mohan, Anup Das and Manab Chakraborty*

Lunar surface properties at both polar and equatorial regions were studied using data from the miniaturized synthetic aperture radar (Mini-SAR) on-board Chandrayaan-1. The Mini-SAR sensor was operated at the S-band (2.38 GHz) with left circular polarization for transmission, and horizontal and vertical polarizations for reception. The returned signal was stored in planetary data system format, where each pixel in an image strip was represented by the corresponding Stokes vectors. The study showed that circular polarization ratio, which is an important parameter that represents scattering associated with planetary ice as well as dihedral reflection, was anomalously high inside some of the craters in the polar regions. Other Stokes parameters such as degree of polarization (m) and LH–LV relative phase (δ) also showed distinctly different types of scattering mechanisms inside and outside the craters on the lunar surface.

Keywords: *Chandrayaan-1* Mini-SAR, circular polarization ratio, lunar craters, Stokes parameters.

THE polarization properties of reflected radar signals contain vital information about the physical and electrical properties of the reflecting surface and subsurface. Surfaces rough at the radar wavelength scale depolarize the incident wave on reflection; thus roughness scale information could be extracted. Similarly, radar interaction with the dielectric properties of the material on a surface provides useful information about the surface types. Hence radar remote sensing of the lunar surface has a unique potential to explore and map lunar resources, especially in the polar regions. The possible existence of water-ice in the lunar polar region has led to the study of the lunar surface and subsurface properties through an orbiting radar. Although the lunar surface is considered to be exceedingly dry, recent radar studies suggest that water-ice may exist in the polar regions. In the late 1970s, James Arnold[1] suggested that impacting comets and water-rich asteroids could add water to the lunar surface. While most of this water would be split by sunlight into its constituent atoms of hydrogen and oxygen and lost into space, some of the water in these objects could migrate to permanently dark areas at the lunar poles, perhaps accumulating to usable quantities.

The possible existence of water-ice deposits in the polar cold traps of the Moon has been a controversial issue since the mid-1990s (ref. 2). The Clementine spacecraft conducted a bistatic radar experiment in 1994, which supported the idea of an ice deposit within the Shackleton crater, near the south pole[3,4]. However, this result generated controversy[5,6], and there is still disagreement whether the observed polarization anomalies are due to ice[7]. However, there is little argument related to the discovery by the Lunar Prospector of enhanced hydrogen levels in the polar regions[8]. The question is whether this hydrogen is in the form of water-ice[2]. While no remote measurement can definitively answer the question of whether ice exists at the lunar poles, an orbiting synthetic aperture radar (SAR) provides the most robust method of obtaining a positive indication of ice deposits. In view of this, a miniaturizer SAR (Mini-SAR) was conceptualized and designed to be put in a lunar polar orbit, so that all permanently shadowed regions will be imaged multiple times by an orbiting radar with incidence angles favourable for determining their scattering properties.

The Mini-SAR was flown on *Chandrayaan-1* launched by the Indian Space Research Organization on 22 October 2008, with an objective to gather data on the scattering properties of the terrain in the polar regions of the Moon. Additionally, SAR was designed to collect information about the scattering properties of the permanently dark areas near the lunar poles at optimum viewing geometry, which are invisible to normal imaging sensors, and thereby detect the presence of water-ice in the permanently shadowed regions on the lunar poles up to the depth of a few metres. Mini-SAR sensor operated at the S-band (2.38 GHz frequency) with transmission in left circular polarization (LCP) and reception in linear horizontal (H) and vertical (V) polarizations. The instrument illuminated the surface of the moon at 35° incidence angle, with a ground range resolution of 150 m and

The authors are in the Space Applications Centre, Ambawadi Vistar P.O., Ahmedabad 380 015, India.
*For correspondence. (e-mail: shivmohan@sac.isro.gov.in)

18 km range swath. A typical image strip consisted of approximately 300 km × 18 km in size.

Mini-SAR data and derived parameters

Mini-SAR data were formatted and stored in a planetary data system (PDS) compliant standard, where each pixel in an image strip consisted of 16 bytes data in four channels of 4 bytes each as $|LH|^2$, $|LV|^2$, Real (LH·LV*) and Imaginary (LH·LV*). The first two channels represent the intensity images for 'horizontal' and 'vertical' receive respectively. The last two channels represent the real and imaginary components respectively, of the complex value for the cross power intensity image between the 'horizontal' and 'vertical' receive. These data were used to derive the Stokes vectors for each pixel equation (1). Several useful quantitative measures follow from the Stokes vectors[9]. Some of the quantitative measures are: degree of polarization (m, representative of polarized and diffuse scattering), circular polarization ratio (CPR, representative of scattering associated with planetary ice and dihedral reflection) and LH–LV relative phase (δ, an indicator of double bounce scattering). Details of the derived Stokes parameters and their significance are shown in Table 1.

$$\begin{pmatrix} S_0 = \langle |\mathrm{LH}|^2 + |\mathrm{LV}|^2 \rangle \\ S_1 = \langle |\mathrm{LH}|^2 - |\mathrm{LV}|^2 \rangle \\ S_2 = 2\Re\langle \mathrm{LH} \cdot \mathrm{LV}^* \rangle \\ S_3 = -2\Im\langle \mathrm{LH} \cdot \mathrm{LV}^* \rangle \end{pmatrix}, \quad (1)$$

where * represents the conjugate of the complex number.

Study area and methodology

The lunar surface is marked by numerous impact craters of different magnitudes as it has been bombarded by meteorites throughout its geological evolution. The craters may be categorized as simple or complex depending upon their size and morphology. Simple craters are bowl-shaped depressions consisting of impact melt and breccia, and are surrounded by a rim of impact ejecta composed of solidified and fragmented rocks and with diameters typically less than 15 km (Figure 1). Complex craters on the other hand, are larger in size and have more complex forms, including shallow, relatively flat floors, central uplifts, and slump blocks and terraces on the inner wall of the crater rim. The complex craters may have a number of simple craters on their floors, called secondary craters.

We studied scattering characteristics of three different areas partly covering Peary, Amundsen and Kopff craters in the lunar north pole, south pole and equatorial regions respectively, using Mini-SAR data. Details of the location of these complex craters are given in Table 2. The Peary and Amundsen craters are known to have numerous secondary craters on their floors that remain permanently dark, whereas the Kopff crater in the equatorial region is sunlit.

The Mini-SAR data were analysed in terms of backscatter and derived Stokes parameters. Radar backscatter was analysed for the effect of surface roughness, whereas polarimetric parameters were used to identify the scattering mechanism. In the absence of suitable calibration factors for the calculation of radar cross-section, the backscatter values were calculated based on logarithmic functions only.

The Mini-SAR data were found to have a LH–LV relative phase (δ) shift of 45° based on our analysis of different portions of the lunar surface. It was assumed that this discrepancy may have been inherited through some system-related errors. In order to overcome this systematic error a phase calibration was done and phase offset of 45° was applied to the Mini-SAR data before further processing.

Results and discussion

Analysis of radar backscatter

Analysis of backscatter at LH and LV polarizations over various features on the lunar surface indicated that LH was generally higher than LV over high backscatter regions which are mostly characterized by blocky ejecta from the craters. The values of both the polarization

Table 1. Derived Stokes parameters and their significance

Stokes parameter	Derivation	Significance
Degree of polarization (m)	$m = \sqrt{(S_1^2 + S_2^2 + S_3^2)} / S_0$	This is an indicator of polarized and diffused scattering; fundamentally related to entropy.
Degree of linear polarization (m_L)	$m_L = \sqrt{(S_1^2 + S_2^2)} / S_0$	This is an indicator of volume versus subsurface scattering.
Circular polarization ratio (CPR)	$\mathrm{CPR} = (S_0 - S_3)/(S_0 + S_3)$	This is an indicator of scattering associated with planetary ice deposits and fresh ejecta.
Relative LH–LV phase (δ)	$\delta = \arctan(-S_3/S_2)$	Sensitive indicator of double bounce scattering.

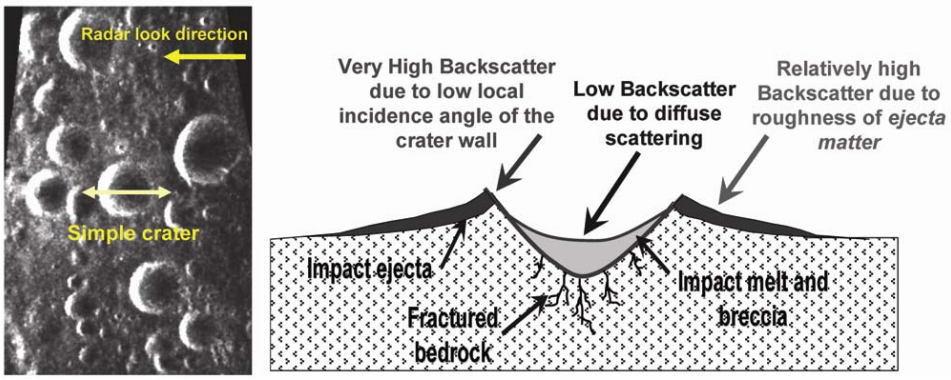

Figure 1. Schematic diagram of a simple impact crater showing relative magnitude of radar backscatter from different zones with respect to Mini-SAR imaging geometry.

Table 2. Details of lunar craters studied

Region	Crater	Location	Crater diameter (km)
Near north pole	Peary	88.6°N, 33.0°E	73
Near south pole	Amundsen	84.3°S, 85.6°E	101
Near equator	Kopff	17.4°S, 89.6°W	41

components were nearly similar in low backscatter regions representing a smooth surface or diffused scattering surface. Table 3 summarizes the dynamic range of LH and LV backscatter (in dB) over different locations as observed from Mini-SAR data.

From Table 3, it is evident that regions inside the lunar craters are characterized by very low radar return due to diffused scattering and the areas over the impact ejecta, which form a rim around the craters show very high radar return due to rough surface scattering. This is in agreement with the structure and composition of the craters as shown in Figure 1. Areas outside the craters, constituting a major part of the lunar surface showed intermediate values of radar backscatter. It was also observed from the analysis that the equatorial region showed higher radar backscatter compared to the polar regions of the lunar surface.

Analysis of Stokes parameters

Stokes parameters as described earlier, are useful tools to study the scattering properties of various features on the lunar surface. The magnitude and sense of polarization of the reflected signal associated with various lunar morphological features as well as water-ice inside the craters were examined using Mini-SAR data. Traditionally, the key parameter used to determine whether ice is present is the CPR. This quantity is equal to the magnitude of the same sense (i.e. the left or right sense of the transmitted circular polarization) divided by the opposite sense polarization signals that are received. CPR was used in the present study to find evidence of subsurface scattering due to dielectric inhomogeneities like water-ice. Volumetric water-ice reflections are known to have CPR greater than unity, whereas surface scattering from dry regolith has CPR less than unity[2]. Apart from CPR, parameters like degree of polarization (m) and relative LH–LV phase (δ) are also important parameters to study the scattering mechanisms associated with lunar regolith. The m–δ together indicate the type of scattering mechanism associated with the target, because at higher m value ($m > 0.5$), δ values close to –90° and +90° indicate surface and double bounce scatterings respectively, and all other values of δ indicate diffused scattering mechanism.

The problem with using CPR alone is that higher values can be obtained from very rough surfaces, such as a rough, blocky lava flow, which has angles that form many small corner reflectors. In this case, the radar signal could hit a rock face (changing LCP into right circular polarization (RCP)), and then bounce over to another rock face (changing RCP back into LCP) and hence to the receiver (Figure 2). This double bounce effect also creates high CPR in that 'same sense' reflections could mimic the enhanced CPR one gets from ice targets[2,10]. Hence, the CPR values estimated from Mini-SAR have been analysed along with m and δ values for indicating the presence of water-ice.

CPR values were calculated along with m and δ for some craters in the lunar polar (Peary crater near the north pole and Amundsen crater near the south pole) and equatorial (Kopff crater) regions and the same were compared with the values outside the craters. Figure 3 shows the LH intensity, CPR, m and δ images and Figure 4 presents the scatter plots showing the relationship between CPR, δ and m inside and outside a few secondary craters on the floor of the Peary crater. High CPR values were found to be associated with regions inside the craters, whereas those outside the craters were low. Also the regions inside the craters showed low m and δ values distributed over –180° to +180°, which are characteristics of diffused

Table 3. LH and LV dynamic range over different locations on lunar surface

Location	LH (in dB)			LV (in dB)		
	Inside crater (max/min)	Outside crater (max/min)	Impact ejecta (max/min)	Inside crater (max/min)	Outside crater (max/min)	Impact ejecta (max/min)
North pole	–13.64/–23.67	–9.02/–20.69	+11.40/–12.99	–14.87/–25.01	–11.45/–22.80	+7.36/–15.86
South pole	–11.37/–28.58	–6.95/–24.81	+5.33/–15.96	–13.62/–29.45	–8.16/–26.57	+2.08/–19.39
Equator	–8.33/–22.56	–3.93/–20.50	+9.57/–9.46	–10.59/–24.95	–5.80/–22.75	+6.74/–15.59

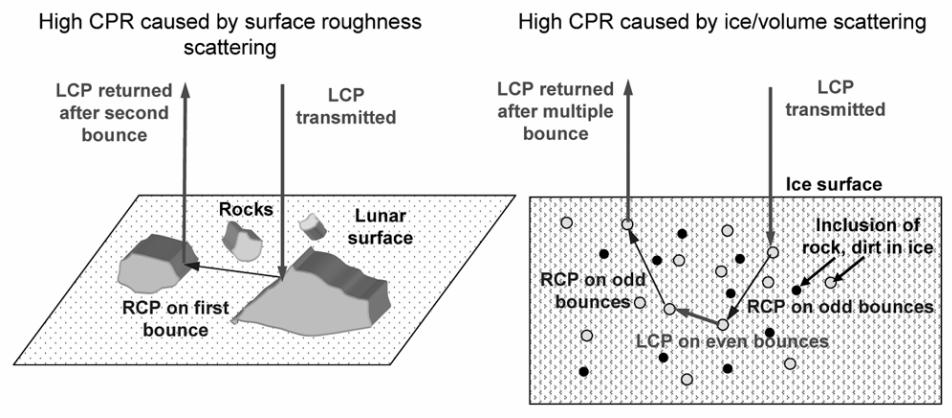

Figure 2. Higher circular polarization ratio (CPR) caused by planetary ice (volume) or roughness due to fresh ejecta (surface) scattering (after Spudis[2]).

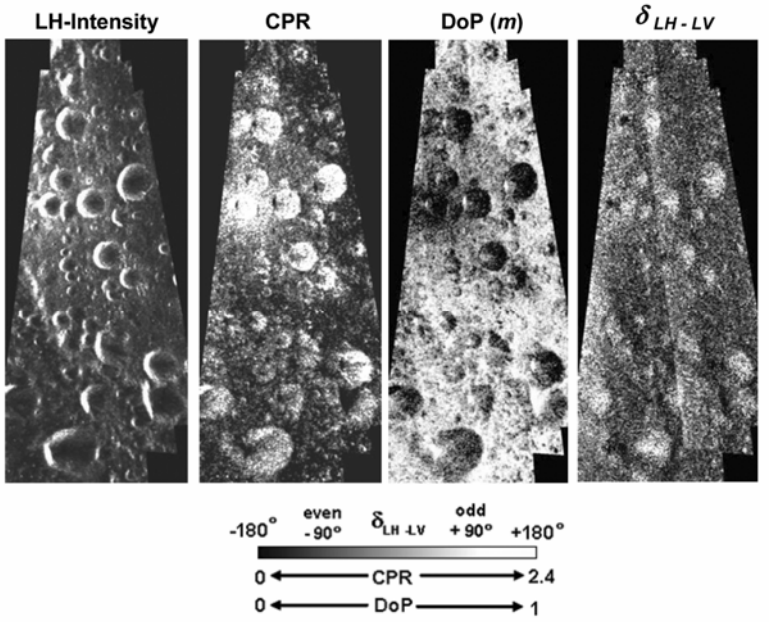

Figure 3. LH intensity, CPR, degree of polarization (m) and relative LH–LV phase (δ) images of a part of Peary crater (88.6°N, 33°E) near the lunar north pole.

or volume scattering. This is indicative of favourable conditions for the presence of water-ice inside these craters.

The same analysis was done for south polar and equatorial craters and the values of total intensity (S_0), CPR, m and δ are given in Table 4. The CPR values were found to be anomalously high inside the secondary craters of Peary and Amundsen in the lunar polar regions (Figure 5). These regions were also associated with diffused scattering mechanisms with lower m values and distributed δ values. This is indicative of the possible presence of

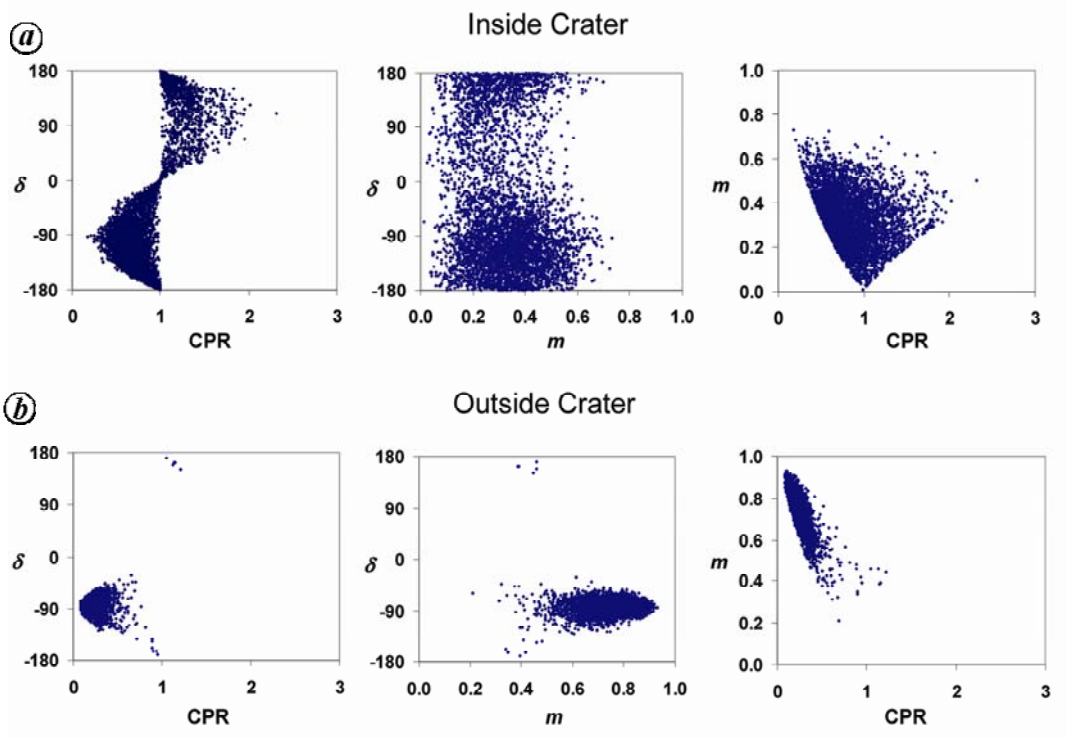

Figure 4. Relationship between CPR, degree of polarization (m) and relative LH–LV phase (δ) associated with targets inside (***a***) and outside (***b***) the crater.

Table 4. Stokes parameters associated with different craters over lunar north pole, south pole and equatorial regions. S_0 indicates the total (LH + LV) intensity

Region	Parameter	S_0 (av.)	m (av.)	δ (av.)	CPR (av.)
North pole (Peary crater)	Inside crater	0.042	0.295 ± 0.12	–38.4°	0.784 ± 0.24
	Outside crater	0.106	0.653 ± 0.18	–87.4°	0.378 ± 0.13
	Impact ejecta	9.663	0.621 ± 0.22	–62.9°	0.430 ± 0.18
South pole (Amundsen crater)	Inside crater	0.121	0.466 ± 0.13	–44.7°	0.710 ± 0.26
	Outside crater	0.341	0.767 ± 0.26	–88.1°	0.231 ± 0.11
	Impact ejecta	6.959	0.868 ± 0.24	–68.3°	0.298 ± 0.12
Equator (Kopff crater)	Inside crater	0.059	0.621 ± 0.15	–93.4°	0.468 ± 0.15
	Outside crater	0.180	0.609 ± 0.21	–76.9°	0.501 ± 0.18
	Impact ejecta	2.532	0.523 ± 0.16	–67.7°	0.559 ± 0.28

water-ice in these secondary craters. Interestingly, regions outside of these craters showed low CPR values, higher m values and average δ values close to –90°, suggesting rough surface scattering from the lunar regolith. The values of Stokes parameters over impact ejecta showed low CPR with high degree of polarization (m) and intermediate values of LH–LV phase difference (δ), indicating contributions from both rough surface and double bounce scattering mechanisms. The impact ejecta are also characterized by very high radar intensities.

For the equatorial crater (Kopff) which is known to be sunlit, the CPR values were found to be uniformly high both inside and outside (Figure 5). These CPR values were however smaller than those found inside the Peary and Amundsen craters in the lunar polar region. The average m and δ values inside and outside the Kopff crater were suggestive of rough surface scattering mechanism as the reason behind elevated CPR in these regions. We also found similar scattering conditions in few of the craters in the polar regions where elevated CPR was found both inside and outside the craters.

Summary and conclusion

The present work is a summary of initial results from Mini-SAR data acquired from the *Chandrayaan-1* mission. The study has brought out a methodology for

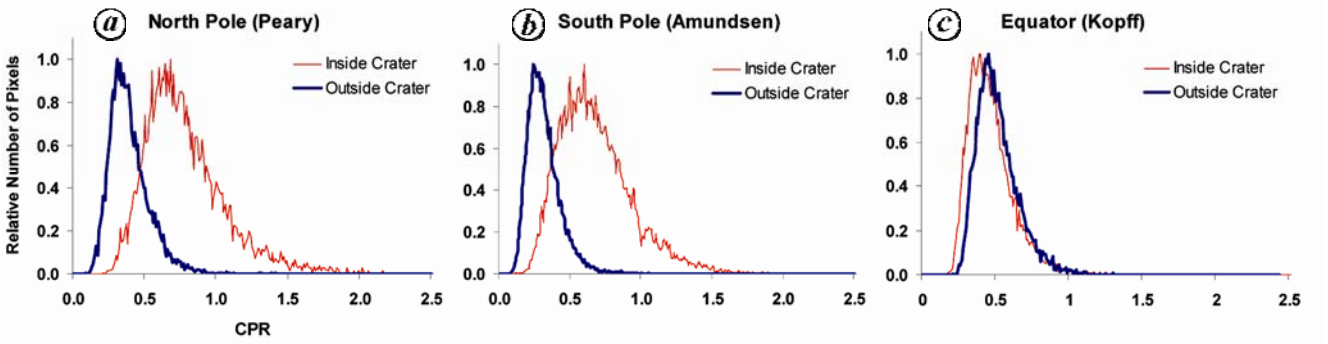

Figure 5. Distribution of CPR inside and outside craters in the north polar (***a***), south polar (***b***) and equatorial (***c***) regions of the Moon.

Mini-SAR data analysis through Stokes parameters. It was found that some of the derived Stokes parameters like CPR, m and δ are effective in characterizing radar scattering associated with lunar surface and subsurface features. The m and δ together characterized the lunar surface in terms of roughness and dominant scattering types, whereas CPR helped in characterizing subsurface scattering due to dielectric inhomogeneities within the scattering volume.

The present study found high CPR values associated with diffused scattering mechanism and low radar backscatter inside a few polar craters believed to be in the permanently shadowed area. This was suggestive of subsurface scattering due to dielectric inhomogeneities like water-ice. Few secondary craters on the floor of the Peary crater near the lunar north pole and the Amundsen crater near the lunar south pole were found to have signatures supporting the presence of water-ice in their interiors. High CPR values were also observed over a few craters in the areas illuminated by sunlight, especially in the equatorial region, but these areas were marked by higher CPR values both inside and outside the craters. This was attributed to scattering from very rough surfaces, such as a rough, blocky lava-flow. Further studies in various other craters are being carried out to find any conclusive evidence for the presence of water-ice in some of the lunar craters.

1. Arnold, J. R., Ice in the lunar polar regions. *J. Geophys. Res.*, 1979, **84**, 5659–5668.
2. Spudis, P. D., Ice on the moon. *Space Rev.*, 2006; http://www.thespacereview.com/article/740/1
3. Nozette, S. *et al.*, The Clementine bistatic radar experiment. *Science*, 1996, **274**, 1495–1498.
4. Nozette, S., Shoemaker, E. M., Spudis, P. D. and Lichtenberg, C. L., The possibility of ice on the Moon. *Science*, 1997, **278**, 144–145.
5. Stacy, N. J. S., Campbell, D. B. and Ford, P. G., Arecibo radar mapping of the lunar poles: A search for ice deposits. *Science*, 1997, **276**, 1527–1530.
6. Simpson, R. A. and Tyler, G. L., Reanalysis of Clementine bistatic radar data for the lunar south pole. *J. Geophys. Res.*, 1999, **104**, 3845–3862.
7. Campbell, D. B., Campbell, B. A., Carter, L. M., Margot, J. L. and Stacy, N. J. S., No evidence for thick deposits of ice at the lunar south pole. *Nature*, 2006, **443**, 835–837.
8. Feldman, W. C., Lawrence, D. J., Elphic, R. C., Barraclough, B. L., Maurice, S., Genetay, I. and Binder, A. B., Polar hydrogen deposits on the Moon. *J. Geophys. Res.*, 2000, **105**, 4175–4195.
9. Raney, R. K., Hybrid-polarity SAR architecture. *IEEE Trans. Geosci. Remote Sensing*, 2007, **45**, 3397–3404.
10. Spudis, P. *et al.*, Mini-SAR: an imaging radar experiment for Chandrayaan-1 mission to the Moon. *Curr. Sci.*, 2009, **96**(4), 533–539.

ACKNOWLEDGEMENTS. We thank Dr R. R. Navalgund, Director, Space Applications Centre (SAC), Ahmedabad for initiating and giving opportunity in Mini-SAR activity. We also thank Prof. J. N. Goswami, Director, Physical Research Laboratory, Ahmedabad for providing Mini-SAR data. Special thanks to Dr R. K. Raney, John Hopkins University, USA and Dr Paul D. Spudis, Lunar and Planetary Institute, Hauston, USA for fruitful discussions, and Dr J. S. Parihar, Deputy Director, Earth, Ocean, Atmosphere, Planetary Sciences and Applications Area (EPSA), SAC, for his valuable suggestions.

Received 7 March 2011; accepted 20 April 2011